The onset of flysch sedimentation in the Kaoko Belt (NW Namibia) – implications for the pre-collisional evolution of the Kaoko–Dom Feliciano–Gariep orogen

Jiří Konopásek[1,2], Karl-Heinz Hoffmann[3], Jiří Sláma[4] and Jan Košler[2,5,*]

[1]*Department of Geosciences, University of Tromsø – The Arctic University of Norway, Dramsveien 201, 9037, Tromsø, Norway*

[2]*Czech Geological Survey, Klárov 3, 118 21, Praha 1, Czech Republic*

[3]*Geological Survey of Namibia, 1 Aviation Road, Windhoek, Namibia*

[4]*Institute of Geology AS CR, v.v.i., Rozvojová 269, 165 00 Praha 6, Czech Republic*

[5]*Department of Earth Science, University of Bergen, Allégaten 41, 5007, Bergen, Norway*

* deceased

Abstract

Detrital zircon provenance study of a metamorphosed sedimentary succession in the eastern part of the Kaoko Belt in Namibia has revealed two distinct sources for the Neoproterozoic sedimentation along the southwestern Congo Craton margin. The lower part of the succession shows detrital zircon ages consistent with erosion of Paleoproterozoic basement of the Congo Craton with an inferred Mesoproterozoic volcano-sedimentary cover. Within the middle part of the succession, which includes glaciogenic sediments correlated with the Sturtian (717–660 Ma) glaciation, the Mesoproterozoic zircon grains disappear and the signal is dominated by ages known from the Congo Craton basement. The sedimentation in these parts of the succession is interpreted as related to the early Neoproterozoic rifting.

The sedimentary rocks in the top part of the profile contain only subordinate proportion of the Paleoproterozoic–Archaean zircon grains and the populations are dominated

by three age groups of *ca.* 1.0–1.2 Ga, *ca.* 800–750 Ma and *ca.* 650 Ma, consistent with erosion of the Punta del Este–Coastal Terrane exposed in the centre of the Kaoko–Dom Feliciano–Gariep orogen. An associated glaciogenic horizon interpreted as reflecting the Marinoan (645–635 Ma) glaciation constrains the sedimentation in the upper part of the succession and suggests a short time span between the high-grade metamorphism/magmatism in the Punta del Este–Coastal Terrane and its exhumation. Sedimentary rocks with such detrital zircon pattern appear also in the Damara and Gariep belts. Their source in the western part of the Kaoko–Dom Feliciano–Gariep orogen suggests that they represent an early orogenic flysch that originated during early collision in the western part of the orogen.

The short time span between the metamorphism/magmatism in the Punta del Este–Coastal Terrane and deposition of the early orogenic flysch derived from it suggests that the Coastal Terrane was never separated from the Congo Craton by an oceanic domain. The estimated time span between the end of lithospheric stretching and sedimentation of the early flysch suggests that the hypothetical Adamastor Ocean separating the western and eastern forelands of the Kaoko–Dom Feliciano–Gariep orogen must have been small.

Key words: Gondwana; Rodinia; Sturtian; Marinoan; Kaoko and Dom Feliciano belts; Rifting

Introduction

The pre-collisional position and extent of separation of the crustal units involved in the formation of the Kaoko–Dom Feliciano–Gariep orogenic system (Fig. 1) is a widely discussed topic (e.g. Porada, 1989; Basei et al., 2005; Goscombe and Gray, 2007; Gray et al., 2008; Frimmel et al., 2011; Konopásek et al., 2014), which has consequences for the reconstruction of the Rodinia and Gondwana supercontinents. Central to such discussion is the position and

extent of a potential oceanic domain, the consumption of which culminated in the formation of the Kaoko–Dom Feliciano–Gariep orogen. The hypothesis of such ocean (Proto-South Atlantic Ocean of Porada, 1979, Adamastor Ocean of Hartnady et al., 1985 or Brazilides Ocean in South American literature) is apparently widely accepted, but its pre-collisional position is unclear due to the lack of evidences for its existence, as would be exhumed blueschist/eclogite facies rocks or ophiolite fragments. Some authors (e.g. Passchier et al., 2002; Oyhantçabal et al., 2009; Chemale et al., 2012) placed the assumed oceanic domain between the Punta del Este–Coastal Terrane (Fig. 1) and the eastern foreland represented by the attenuated Congo Craton margin in the north and the western edge of the Kalahari Craton in the south. Consequently, such configuration implies the Neoproterozoic suture on the eastern side of the Kaoko–Dom Feliciano–Gariep orogen. Other authors (e.g. Basei et al., 2000; Goscombe and Gray, 2007; Frimmel et al., 2011) placed the oceanic domain between the Punta del Este–Coastal Terrane and the western foreland represented by the Nico Perez–Luis Alves terranes in Uruguay and southeastern Brazil (Fig. 1). Solution of this ambiguity requires data that allow an interpretation of the measure of the pre-convergence separation of the Punta del Este–Coastal Terrane from the foreland domains of the Kaoko–Dom Feliciano–Gariep orogen.

In our previous work we have presented evidence for proximity of the Coastal Terrane and the attenuated Congo Craton margin in the Kaoko Belt between *ca.* 650 Ma and the time of their mutual collision at *ca.* 580 Ma (Konopásek et al., 2014). This evidence is based on the zircon provenance data from the upper part of the high-grade metamorphosed sedimentary succession covering the Congo Craton basement of the Orogen Core unit and northwestern Central Kaoko Zone, which point to the Coastal Terrane as the most likely source of the clastic sediments laid down in that time span. However, as the upper sedimentary succession

described in that study is devoid of syn-sedimentary volcanic units that would allow dating of the sedimentation, the exact timing of the Costal Terrane erosion remained unconstrained.

Within the southeastern Central Kaoko Zone (Fig 1), a thick folded but stratigraphically continuous low- to medium-grade basinal succession is composed of mainly coarse- to fine-grained clastic and minor carbonate sedimentary rocks and local volcanic rocks with low grade of metamorphic overprint (Fig. 2). The middle part of the succession contains weakly metamorphosed thick glaciogenic diamictite with shale and thin limestone correlated with the Chuos Formation of the middle Otavi Group carbonate platform sequence of the Eastern Kaoko Zone (Figs 2 and 3; Guj, 1970). The presence of a second thin glacial interval, consisting of ice-rafted debris correlated with the Ghaub Formation of the upper Otavi Group has recently been identified from new field mapping within the upper succession. The glacial units are correlated with the global Sturtian (717–660 Ma; Macdonald et al., 2010; Rooney et al., 2014; 2015) and Marinoan (< 645–635 Ma; Hoffmann et al., 2004; Condon et al., 2005; Rooney et al., 2015; Prave et al., 2016) glacial episodes respectively, and thus provide a reliable age model for the timing and duration of sedimentation of the middle and upper sedimentary successions.

In this contribution we present new detrital zircon age spectra from this continuous and stratigraphically well-constrained succession of the southeastern Central Kaoko Zone. Such data allow correlation of the studied low-grade Neoproterozoic units with the high-grade metasedimentary rocks in the western part of the Kaoko Belt, and also with the clastic sedimentation in the basinal part of the Damara Orogen. Moreover, the data provide robust arguments for the discussion of the pre-collisional position of the Punta del Este–Coastal Terrane with respect to the hypothetical Adamastor/Brazilides Ocean, as well as other crustal blocks involved in the assembly of western Gondwana along the Kaoko–Dom Feliciano–Gariep orogenic system.

Geological setting

The Kaoko Belt in northwestern Namibia consists of two principal tectonic units. The major part of the belt is an attenuated margin of the Archaean–Mesoproterozoic Congo Craton (Seth et al., 1998; S. Kröner et al., 2004; A. Kröner et al., 2010; 2015) with its Neoproterozoic sedimentary cover (Guj, 1970; Dingeldey et al., 1994; Prave, 1996; Hoffman and Prave, 1996; Goscombe, 1998a,b; Konopásek et al., 2014). The overriding tectonic unit is the Coastal Terrane (Fig. 1; Goscombe et al., 2005; Goscombe and Gray, 2007).

The attenuated Congo Craton margin is subdivided into three zones with different styles of deformation and metamorphic grade (Miller, 1993; Goscombe et al., 2005). Its western part represents the Orogen Core unit (Goscombe et al., 2005) showing granulite-facies metamorphism and extensive partial melting at *ca.* 550 Ma (Goscombe et al., 2005; Konopásek et al., 2008). Farther to the east and in the tectonic footwall is the Central Kaoko Zone (Miller, 1993), which is a thrust and fold belt with slices of the basement incorporated into its metamorphosed and deformed sedimentary cover. Dating of volcanic rocks and detrital zircon grains in the host sedimentary rocks has shown that the metasedimentary part of the Central Kaoko Zone is built of two distinctively different successions (Konopásek et al., 2014). The sedimentation associated with volcanic activity in the lower part of the succession took place between at least *ca.* 740 and 710 Ma. The sedimentary age of the upper part is between *ca.* 650 and 580 Ma, where the upper limit is set by the age of an early metamorphism of this unit (Goscombe et al., 2003). Due to the metamorphism and deformation, it is not clear whether there has been any sedimentary unconformity present between these two successions. The whole unit has developed an inverted Barrowian-type metamorphism and the grade decreases towards the east (Goscombe et al., 2003; Will et al., 2004). The Central Kaoko Zone was thrust along the Sesfontein Thrust (Fig. 2) over the very

low grade Eastern Kaoko Zone represented by the western edge of the Otavi Group carbonate platform and overlying molasse sedimentary rocks of the Mulden Group (Guj, 1970; Prave, 1996; Hoffmann and Prave, 1996). The Otavi Group contains two regional glacial diamictite units, the lower Chuos Formation and the upper Ghaub Formation (Hoffmann and Prave, 1996; Hoffman and Halverson, 2008).

The Coastal Terrane shows markedly different evolution with respect to the underlying Congo Craton margin. There is apparently no pre-Neoproterozoic basement exposed in the Coastal Terrane and the pre-collisional rock association is represented by metamorphosed clastic sedimentary rocks with intercalated quartz-feldspathic gneisses and amphibolites. The gneisses and amphibolites have been interpreted as former syn-sedimentary bimodal volcanic rocks and dated at *ca.* 800 Ma (Konopásek et al., 2008). The volcano-sedimentary succession was migmatized at *ca.* 650–630 Ma (Franz et al., 1999; Goscombe et al., 2005; Konopásek et al., 2008) and this partial melting event was associated with an intrusion of small portions of magmatic rocks (Seth et al., 1998; S. Kröner et al., 2004). After the migmatization, but still prior to the thrusting over the Congo Craton margin, the Coastal Terrane was intruded by basic–intermediate and felsic plutonic rocks of the Angra Fria Magmatic Complex now exposed in the NW part of the unit. The ages of the intrusions show two time intervals, where the older suite intruded at *ca.* 625–620 Ma and the younger suite at *ca.* 585–575 Ma (Konopásek et al., 2016). The metamorphic and magmatic history of the Coastal Terrane and the Angra Fria Complex coincides with that recognized in the Punta del Este Terrane and the Florianópolis Batholith of the Dom Feliciano Belt in South America, respectively (Gross et al., 2009; Oyhantçabal et al., 2009; Lenz et al., 2011). This allowed establishment of an improved spatial link between the geological units of the Kaoko and Dom Feliciano belts (Konopásek et al., 2016).

In the final stage of its evolution, the Coastal Terrane was thrust obliquely over the Congo Craton margin between *ca*. 580 and 550 Ma (Goscombe and Gray 2007; Ulrich et al., 2011). The thrusting was accompanied by intrusions of a large number of magmatic bodies with ages spanning the whole time interval of thrusting (Seth et al., 1998; S. Kröner et al., 2004; Masberg et al., 2005; Konopásek et al., 2008; Janoušek et al., 2010).

Sedimentary succession of the study area

The rocks studied in this work represent a Neoproterozoic sedimentary cover of the Congo Craton basement in the easternmost part of the Central Kaoko Zone (Figs 2 and 3). The Neoproterozoic succession was folded with various intensity and metamorphosed under the lower greenschist-facies conditions (Guj, 1970; Dingeldey et al., 1994).

The succession starts with coarse-grained clastic sedimentary rocks of the Nosib Group directly overlying the Archaean–Paleoproterozoic basement of the Congo Craton. The Nosib Group rocks are overlain by a thick succession of fine- to medium-grained schists and quartzites with dolomite and limestone beds in the lower part and mainly calcareous quartzite and micaceous quartzites interbedded with schists in the upper part. Both the lower and upper parts were intruded by small bodies (or apophyses of a larger body) of a coarse-grained metagabbro (Figs 2 and 3). Above the quartzites there is a unit of mafic volcanic rock metamorphosed to greenschist followed by a thick succession of glaciogenic, medium-grained clastic sedimentary rocks with centimetre- to decimetre-sized polymict basement and minor carbonate clasts and with high proportion of iron oxides. This glaciogenic succession is correlated with the Chuos Formation diamictite of the Otavi Group (Fig. 3) and interpreted as representing the Sturtian (717–660 Ma) global glaciation. The diamictite of the Chuos Formation is overlain by an intercalation of fine- and medium-grained clastic

metasedimentary rocks and these pass gradationally into a thick succession of metagreywacke with subordinate carbonate beds.

A thin unit consisting of laminated, weakly metamorphosed pelite with rare, pebble- to boulder-sized lonestones, interpreted as ice-rafted clasts (dropstones), and sharply overlain (capped) by thin (10–15 cm) dark rusty brown weathering medium grey dolostone, forms a laterally continuous unit within the middle part of the greywacke succession (Fig. 3). This is followed by thinly interbedded dolostone and metapelite and grey limestone. The dropstone-bearing pelite and cap dolostone are correlated with the Ghaub Formation and overlying cap dolostone (Keilberg Member) of the Otavi Group and therefore interpreted as representing the Marinoan (*ca.* 645–635 Ma) glaciation (Hoffmann et al., 2004; Prave et al., 2016).

Description of samples and results of U–Pb detrital zircon dating

U–Pb ages of the zircon populations were determined by laser ablation inductively coupled plasma mass spectrometry (LA–ICP–MS) and the isotopic data are given in the electronic appendix. Reported zircon U–Pb concordia age spectra (Figs 4, 5 and 6a) comprise only analyses with 2σ uncertainty ≤ 10 % and probability of concordance ≥ 1 %. The frequency of zircon age populations is presented in form of histograms and kernel density estimate of Vermeesch (2012). Description of zircon separation and analytical method is provided in the Appendix.

Sample NL 20

Sample NL 20 (S19°10.894', E13°34.886' – all coordinates are WGS 84) is a carbonate-bearing feldspathic quartzite with an accessory opaque mineral collected from the lower part of a unit of schists and quartzites overlying the basal Nosib Group (Figs 2 and 3). The zircon grains are mostly *ca.* 100–150 μm long, oval in shape and some of them show

relic morphology of prismatic crystals with abraded edges. Cathodoluminescence (CL) imaging of the grains revealed mostly the presence of oscillatory zoning that is in numerous grains truncated at the edges, probably due to abrasion during transport. Smaller proportion of grains revealed sector zoning or no zoning at all.

Isotopic dating yielded data with the probability of concordance ≥ 1 % and 2σ uncertainty ≤ 10 % for 83 zircon grains. The results of dating are plotted in Fig. 4a, where the corresponding spectrum of dates shows the highest proportion distributed around a peak at *ca.* 1.80 Ga. The remaining analyses form a broad peak centred at *ca.* 1.30 Ga, which represents clusters of data between *ca.* 1.00 and 1.50 Ga. Some individual data appear also in the interval *ca.* 1.95–2.75 Ga.

Sample NL 24B

Sample NL 24B (S19°19.908', E13°35.702') is a carbonate-bearing micaceous quartzite occurring directly below the layer of metamorphosed volcanic rock (Figs 2 and 3). The quartzite contains the mineral assemblage quartz-carbonate-plagioclase-microcline-biotite-chlorite-white mica with accessory tourmaline and opaque mineral. Zircon crystals extracted from this sample mostly show relic prismatic crystal shape, some of them are more rounded and show oval shapes. Grains are *ca.* 80–200 μm long, mostly with well visible oscillatory zoning in CL. Again, small number of grains is CL-bright with sector or convolute zoning and some show CL-bright rims with embayments into the oscillatory-zoned parts.

Analysis of 98 grains provided data with the probability of concordance ≥ 1 % and 2σ uncertainty ≤ 10 %. The spectrum of concordia ages is presented in Fig. 4b and shows several peaks at *ca.* 1.85, 1.70, 1.40, 1.20 and 1.05 Ga, as well as some individual data at *ca.* 950 Ma and between 2.00 Ga and 2.20 Ga.

Sample NL 21

Sample NL 21 (S19°13.233', E13°34.937') is a quartzite occurring within the metavolcanic unit (Figs 2 and 3). The quartzite contains white mica, carbonate, plagioclase, microcline, chlorite, opaque mineral and epidote. Zircon grains extracted from this sample are either ovoid in shape or show well preserved prismatic crystals. The grains are *ca.* 100–150 μm long and most of them show oscillatory zoning in CL, nevertheless the proportion of sector-zoned crystals is apparently higher than in the previous two samples. Some grains show again distinct CL-bright rims with embayments into the darker parts of the crystal.

Analysis of 98 grains yielded data with the probability of concordance ≥ 1 % and 2σ uncertainty of ≤ 10 %. The dates form two maxima at *ca.* 1.75 and 1.85 Ga and there is also a small number of individual data at *ca.* 900 Ma, between 1.30 and 1.60 Ga, around 2.00 Ga and at 2.50 Ga (Fig. 4c).

Sample NL 26

Sample NL 26 (S19°28.076', E13°34.505') is a quartzite collected directly below the lower diamictite horizon of the profile (Figs 2 and 3). The sample is strongly foliated and bears the mineral assemblage quartz-muscovite-biotite-plagioclase-carbonate with accessory titanite and opaque mineral. Zircon occurs as prismatic crystals *ca.* 100–200 μm long with various degrees of abrasion of the edges. CL imaging of the grains revealed mostly oscillatory zoned crystals and numerous crystals with complex internal structures. As in the previous samples, several zircon grains show CL-bright, ca. 10 μm wide rims with embayments into darker, often oscillatory zoned parts of the crystals.

Isotopic dating yielded data with the probability of concordance ≥ 1 % and 2σ uncertainty ≤ 10 % for 92 zircon grains. The resulting spectrum (Fig. 4d) is very similar to that observed in the sample NL 21 (Fig. 4c). The calculated concordia ages cluster around

1.75 and 1.85 Ga and there is a small number of individual dates around 1.20 and 2.00 Ga and at *ca.* 2.60 and 2.80 Ga.

Sample NL 25

Sample NL 25 (S19°27.492', E13°35.108') represents the lower glaciogenic unit interpreted as the Chuos Formation diamictite (Figs 2 and 3). In the hand specimen, the sample is composed of centimetre- to decimetre-sized carbonate clasts surrounded by medium-grained rusty-brown matrix suggesting a high proportion of iron oxide. In the thin section made from the matrix, the rock is composed by *ca.* 30% of opaque mineral accompanied by quartz, plagioclase, biotite, carbonate and subordinate chlorite. Zircon in this sample are mostly *ca.* 50–150 μm large fragments of ovoid or prismatic grains. Majority of them show oscillatory zoning in CL, some grains have numerous fractures and sometimes show CL-bright regions around them.

Dating of zircon from this sample yielded 96 concordia ages with the probability of concordance ≥ 1 % and 2σ uncertainty of ≤ 10 %. The vast majority of the data forms a peak around 1.85 Ga. There is another group of dates clustering around *ca.* 1.70 Ga and the rest are individual data in the interval 900 Ma – 1.50 Ga and several data around 2.50–2.60 Ga (Fig. 4e).

Sample MDB-6

The lower diamictite horizon is overlain by weakly metamorphosed pelitic sedimentary rocks (Figs 2 and 3), which alternate with more psamitic rocks and the metamorphosed psamite is the sample MDB-6 (S19°29.715', E13°26.783'). The sample consists of *ca.* 0.5–1 mm large, partly recrystallized clasts of plagioclase and quartz surrounded by finer-grained matrix made of recrystallized quartz, feldspar, carbonate mineral,

muscovite, biotite, chlorite and an opaque mineral. Analysed zircon grains are *ca.* 70–180 μm large. Most of them show well-developed concentric oscillatory zoning in CL and only minor proportion of the crystals shows ill-defined oscillatory or sector zoning.

Isotopic dating provided 107 dates with the probability of concordance ≥ 1 % and 2σ uncertainty ≤ 10 %. The data show a single peak centred at *ca.* 1.80 Ga and individual data at *ca.* 1.00, 1.50 and between *ca.* 1.90 and 2.20 Ga (Fig. 4f).

Sample NL 27

The uppermost part of the sampled sedimentary succession is represented by a unit of weakly metamorphosed greywacke with subordinate dolomite beds. This unit contains the upper glaciogenic horizon (Figs 2 and 3) that is interpreted as the Marinoan (*ca.* 645–635 Ma) Ghaub Formation diamictite. The greywacke sample NL 27 (S19°34.197', E13°27.036') was collected at the bottom of this unit and its mineralogy is mostly represented by quartz and carbonate together with high proportion of opaque mineral, white mica, subordinate plagioclase feldspar, biotite and tourmaline. Zircon crystals extracted from this sample are mostly *ca.* 120–150 μm long and show various shapes and patterns in CL. Large proportion of grains is short or long prismatic with preserved crystal faces and well developed oscillatory zoning. Other grains do not have well defined crystal shape, they are oval and show truncated oscillatory zoning. Finally, *ca.* 10% of grains show irregular or ovoid shapes or fragments of crystals with sector or faint and irregular zoning in CL.

Analysis of 73 grains yielded data with the probability of concordance ≥ 1 % and 2σ uncertainty of ≤ 10 %. The dates form two maxima at *ca.* 1.05 Ga and *ca.* 800 Ma, but the later one in fact represents a group of dates between *ca.* 650 and 850 Ma. A small number of individual data appear at *ca.* 1.65 Ga, between 1.85 and 2.00 Ga and at 2.65 Ga (Fig. 5a).

Sample MDB-5

Sample MDB-5 (S19°28.725', E13°24.715') comes from the same unit of metagreywackes as the sample NL 27, but from the position directly below the Ghaub Formation diamictite (Figs 2 and 3). The sample MDB-5 consists of quartz, feldspar, carbonate mineral, muscovite, chlorite, biotite, opaque mineral and accessory tourmaline. CL imaging of the zircon grains revealed large variety of grain shapes from long (>200μm) prismatic with well-defined crystal shapes through short prismatic up to ovoid (*ca.* 90μm large), strongly abraded grains with clearly truncated oscillatory zoning. Most of the zircon crystals show concentric or non-concentric oscillatory zoning, but large proportion of the grains have faint, patchy or sector zoning and some of them are featureless in CL.

Dating of zircon extracted from the sample MDB-5 provided 114 dates with the probability of concordance ≥ 1 % and 2σ uncertainty of ≤ 10 % and they cluster in two broad peaks centred at *ca.* 700 Ma and *ca.* 1.05 Ga. Minor number of analyses provided data with calculated concordia ages between *ca.* 1.75 and 2.00 Ga and one concordia age at 2.60 Ga (Fig. 5b).

Samples HKB-1 and NL 29

Samples HKB-1 (S19°34.785', E13°25.678') and NL 29 (S19°34.738', E13°25.601') were collected from the metagreywackes overlying the Ghaub Formation diamictite horizon (Figs 2 and 3). The samples consist mostly of quartz, plagioclase feldspar and carbonate, together with smaller amount of muscovite, biotite, chlorite, opaque mineral and subordinate tourmaline. The shape and internal features of zircon crystals in HKB-1 are similar to those observed in the sample HKB-5. Zircon grains separated from the sample NL 29 are mostly

long prismatic with euhedral crystal shapes and lengths of *ca.* 150–270 μm. Such grains mostly show concentric oscillatory zoning in CL. Small proportion of grains is short prismatic or ovoid in shape but also with well-developed concentric zoning. Only individual grains have irregular shapes and these usually show complicated internal textures in CL like convolute or patchy zoning or they have no zoning at all.

Sample HKB-1 yielded 108 dates with the probability of concordance ≥ 1 % and 2σ uncertainty of ≤ 10 %. The data show one broad peak between *ca.* 950 and 1.15 Ga and one broad group of data between *ca.* 600 and 800 Ma with two peaks at 650 and 700 Ma. There are also some individual data at *ca.* 1.90 and 2.70 Ga (Fig. 5c).

Isotopic analysis of zircon in the sample NL 29 yielded 85 concordia ages with the probability of concordance ≥ 1 % and 2σ uncertainty of ≤ 10 %. The dates concentrate in two time intervals, where one group represents dates between *ca.* 1.00 and 1.25 Ga with a peak at *ca.* 1.05 Ga, and the other between *ca.* 650 and 850 Ma with two well-defined peaks at *ca.* 650 and 800 Ma. Only four analyses provided dates older than 1.40 Ga (Fig. 5d).

Sample NM 32

Sample NM 32 (S19°12.438', E13°50.464') is a weakly metamorphosed pelitic sediment collected in the Eastern Kaoko Zone east of the main study area (Fig. 2). This rock represents the molasse sediments of the Mulden Group consisting of alternation of quartz- and white mica + chlorite-rich layers and the other mineral phases are epidote and accessory opaque mineral. Nearly all of the zircon crystals extracted from the sample are long prismatic with length between *ca.* 120 and 200 μm and only subordinate number is short prismatic with length of *ca.* 100 μm. Most of the grains show well-developed concentric or nonconcentric oscillatory zoning in CL and only small number of them show sector or convolute zoning.

Isotopic dating yielded data with the probability of concordance ≥ 1 % and 2σ uncertainty ≤ 10 % for 65 zircon grains. The data are plotted in Fig. 6c and the resulting spectrum shows the highest proportion of dates distributed around a peak at *ca.* 600 Ma. The remaining analyses form two smaller peaks centred at *ca.* 800 Ma and 1.05 Ga. Some individual data appear in the age interval between *ca.* 1.90 and 2.10 Ga.

Sm-Nd isotopes

In order to further characterize possible sources of the detritus for the samples, we have analysed Nd isotopic compositions in four samples from the lower and middle parts, and in four samples from the top of the studied stratigraphic interval. The new Nd isotopic analyses are presented in Tab. 1 together with previously published data from the rocks representing the Neoproterozoic metasedimentary units of the Kaoko Belt. Some of the published Sm/Nd ratios from metasedimentary samples collected in migmatitic units (Goscombe et al., 2005; Jung et al., 2007) are markedly different from those typical of the average continental crust. Thus, the depleted-mantle Nd model ages were calculated using the two-stage Nd evolution model of Liew and Hofmann (1988) assuming a major Sm/Nd fractionation during the last high-grade metamorphic event in the study area, i.e. at *ca.* 550 Ma. The two-stage Nd model ages obtained for samples from the bottom part of the stratigraphic interval (NL 21 and NL 24 B) are 2.39 and 2.17 Ga, respectively. Samples from the middle part of the profile (NL 25 and MDB-6) yielded the Nd model ages of 1.85 and 1.98 Ga and the samples from the stratigraphic top of the profile (NL 27, NL 29, HKB-1 and and MDB-5) show the Nd model ages of 1.45, 1.56, 1.46 and 1.40 Ga, respectively.

Discussion

1. Detrital zircon age patterns of the clastic sediments in the eastern part of the Kaoko Belt

The detrital zircon data show four different patterns. First pattern appears in the samples NL 20 and NL 24B (Fig. 4a,b), where the data apparently cover the entire time interval between *ca.* 1.00 and 2.00 Ga with one group of dates between *ca.* 1.70 and 1.85 Ga and another group straddling a larger time interval between *ca.* 900 Ma and *ca.* 1.40 Ga. The samples NL 21, NL 26, NL 25 and MDB-6 (Fig. 4c, d, e, f) represent the second group. Here, the vast majority of the dates appears only in the age interval *ca.* 1.70–1.85 Ga. The third age pattern comes solely from the samples collected in the uppermost greywacke unit of the sedimentary succession, i.e. the samples NL 27, HKB-1, MDB-5 and NL 29 (Fig. 5). Their detrital zircon age spectra show a bimodal distribution with one group of dates in the interval *ca.* 900 Ma – 1.20 Ga and another group in the interval *ca.* 630–850 Ma. The last age pattern shows the dates obtained from the detrital zircon population of the sample NM 32 (Fig. 6c) representing the Mulden Group in the Eastern Kaoko Zone. The pattern itself is similar to that observed in the previous group, but in the sample NM 32 the largest number of dates appears around *ca.* 600 Ma.

The presence of clastic zircon with dates ≤ 1.00 Ga in the samples from the lower part of the studied succession confirms its Neoproterozoic age. The dates from the samples NL 20 and NL 24B differ from those recorded in the samples NL 21, NL 25, NL 26 and MDB-6 by substantial suppression of the Mesoproterozoic dates in the latter group (Fig. 4). The detrital zircon concordia age patterns in these two groups of samples suggest a permanent availability of *ca.* 1.75–2.0 Ga old source. This is no surprise, as the (meta)granitoid rocks of this age dominate the underlying Congo Craton basement (Seth et al., 1998; S. Kröner et al., 2004; A. Kröner et al., 2010; 2015; Kleinhanns et al., 2015). The Mesoproterozoic dates between *ca.* 1.4 and 1.0 Ga appear in a large number in the samples from the lower part of the studied stratigraphic interval (NL 20 and NL 24B; Fig. 4a,b) and their disappearance towards the

higher stratigraphic levels suggests gradual erosion of source rocks with Mesoproterozoic zircon. Rocks with ages between 1.4 and 1.0 Ga are not common in the Congo Craton basement and the only occurrence of metamorphosed Mesoproterozoic igneous rocks is known from the northern Kaoko Belt (A. Kröner, pers. comm.). It is however possible that a volcanosedimetary series of this age covered this part of the craton before the onset of the Neoproterozoic rifting and was eroded during ongoing crustal extension. An alternative source of the detrital material for the lower part of the studied sedimentary succession are the Mesoproterozoic rocks of the Namaqua Metamorphic Complex and the Rehoboth Inlier along the northwestern and western edge of the Kalahari Craton (Fig. 1; Becker et al., 2006), which may have been in close proximity with the Congo Craton at the onset of the Neoproterozoic rifting.

Samples from below and above the recently identified Marinoan glaciogenic unit of the Ghaub Formation within the upper sedimentary succession of the southeastern Central Kaoko Zone show markedly different detrital zircon age patterns than the samples collected in the lower stratigraphic positions. The populations in all four dated samples (NL 27, NL 29, HKB-1 and MDB-5; Fig. 5) are dominated by the late Mesoproterozoic – early Neoproterozoic zircon grains, whereas the Paleoproterozoic dates are scarce. The lack of the Paleoproterozoic dates and an overall presence of the *ca.* 650 Ma zircon in these samples rules out the Congo or Kalahari cratons and their Neoproterozoic sedimentary cover as the source rocks. This is because the *ca.* 650 Ma felsic–intermediate igneous rocks that could have provided zircon of this age are not known from any of the tectonic units of the Kaoko, Damara or Gariep belts with the Congo or Kalahari cratonic basement. The closest tectonic unit with the demonstrated presence of *ca.* 650 Ma igneous and high-grade metamorphic activity is the Coastal Terrane in the Kaoko Belt and its equivalent, the Punta del Este Terrane, in the Dom Feliciano Belt (Seth et al., 1998; Franz et al., 1999; Goscombe et al.,

2005; Konopásek et al., 2008; Oyhantçabal et al., 2009; Lenz et al., 2011). Apart from the *ca.* 650 Ma plutonic activity and associated granulite-facies metamorphism, the Punta del Este–Coastal Terrane contains an important proportion of metamorphosed felsic–intermediate igneous rocks dated between *ca.* 800 and 770 Ma (Konopásek et al., 2008; Oyhantçabal et al., 2009; Lenz et al., 2011; Basei et al., 2011; Masquelin et al., 2012). These ages correspond well with the Neoproterozoic zircon populations older than *ca.* 650 Ma found in the samples NL 27, NL 29, HKB-1 and MDB-5. Finally, inherited zircon grains dated in some of the Neoproterozoic igneous rocks of the Punta del Este–Coastal Terrane show almost exclusively mid–late Mesoproterozoic (*ca.* 1.30–0.95 Ga) ages (Lenz et al., 2011; Basei et al., 2011; Masquelin et al., 2012), which is in agreement with the late Mesoproterozoic zircon populations observed in all four samples from this stratigraphic position. All these facts point to the Punta del Este–Coastal Terrane as the most likely source for the samples NL 27, NL 29, HKB-1 and MDB-5.

Three zircon grains in the sample HKB-1 collected above the diamictite horizon of the Ghaub Formation yielded dates of *ca.* 600 Ma. Although all of them fulfil the criterion for considering them as concordant or nearly concordant analyses, two of them have a low probability of concordance (1 and 19%) and the third grain we consider as outlier that says little about the maximum depositional age of the sample protolith. The other youngest dates (22 data) cluster around an age of 630 Ma (weighted average of concordia ages is 629 ± 4 Ma), which we consider as the best estimate of the age of the youngest zircon population in the sample HKB-1. The youngest zircon population in the sample NL 29 from an equivalent stratigraphic positions does not show dates younger than *ca.* 630 Ma and the weighted average of concordia ages for the 13 youngest dates is 652 ± 6 Ma.

The differences in sources for the sedimentation of the lower, middle and upper part of the studied profile are reflected also by different Nd model ages of the samples (Tab. 1). The

samples NL 21 and NL 24B from the lower part of the profile show early Paleoproterozoic model ages (2 stage T^{Nd}_{DM} of 2.39 and 2.17 Ga, respectively), whereas the model ages of the samples NL 25 and MDB-6 in the middle part of the profile are slightly younger (2 stage T^{Nd}_{DM} of 1.85 and 1.98 Ga, respectively). In contrast to that, the samples from the upper part of the profile (NL 27, NL 29, HKB-1 and MDB-5) show younger, mostly Mesoproterozoic model ages between 1.56 and 1.40 Ga, which is another evidence that rules out the Paleoproterozoic basement of the Congo Craton as a source region. These data are consistent with the previous observations made in other parts of the Neoproterozoic sedimentary cover in the Kaoko Belt (see summary in Tab. 1)

The sample NM 32 of the late orogenic molasse sediments from the Eastern Kaoko Zone shows generally the same detrital zircon age signals as the samples from the uppermost strata of the Central Kaoko Belt succession. The major difference is the suppression of late Mesoproterozoic dates and the dominance of Neoproterozoic dates with two peaks at *ca.* 800 Ma and at *ca.* 600 Ma. As discussed above, the dates between *ca.* 800 and 630 Ma represent the typical Punta del Este–Coastal Terrane signal. Large proportion of grains dated at *ca.* 600 Ma suggests initial erosion of magmatic rocks intruded along the western edge of the Punta del Este–Coastal Terrane represented by the Aiguá, Pelotas and Florianópolis batholiths in the Dom Feliciano Belt and the Angra Fria Complex intruding the Coastal Terrane in the Kaoko Belt (see summary in Konopásek et al., 2016).

2. Comparison of the results with the data from the high-grade part of the Central Kaoko Zone

The presence of the Sturtian (*ca.* 717–660 Ma) and Marinoan (*ca*. 645–635 Ma) glacial intervals recognized within the tectonically uninterrupted and well documented

stratigraphic succession of the southeastern Central Kaoko Zone, provide important age constraints for comparison and improved correlation with previously published detrital zircon data from the medium – high-grade metasedimentary succession of the Kaoko Belt in which the glaciogenic units appear to be absent or have not been recognized (Konopásek et al., 2014). Such comparison shows that the sample of the basal Neoproterozoic Nosib Group quartzite (sample NI 177 in Fig. 4 of Konopásek et al., 2014) yielded zircon age spectrum very similar to the samples from the lower part of the stratigraphic section (samples NL 20 and NL 24B in Fig. 4) dated in this work. Goscombe et al. (2005) also reported comparable spectrum of detrital zircon ages from a quartzite of the Hartmann Group in the northern Kaoko Belt.

Samples from the quartzites overlying the basement in the Central Kaoko Zone and in the Orogen Core domain (samples NK 54 and NI 128, respectively, in Fig. 4 of Konopásek et al., 2014) show one zircon population between *ca.* 1.70 and 2.00 Ga and another population with Mesoproterozoic dates between *ca.* 1.20 and 1.50 Ga. We also consider the detrital zircon signals in these samples as equivalent to samples NL 20 and NL 24B presented in this work and the only difference is the appearance of *ca.* 950 Ma – 1.10 Ga zircon dates in the later samples.

Zircon age populations in samples from the upper part of the medium to high-grade cover of the Kaoko Belt (samples NI 133, NL 15 and NH 059 in Fig. 4 of Konopásek et al., 2014) match with the age spectra from rocks representing the top of the sedimentary succession at the eastern edge of the Central Kaoko Zone (samples NL 27, NL 29, HKB-1 and MDB-5; Fig. 5). These samples have zircon populations with dominant late Mesoproterozoic – early Neoproterozoic dates and the Paleoproterozoic zircon dates are present only sporadically. The only exception is the sample NH 059, where the proportion of Paleoproterozoic and even Archean zircon is high.

The sample NM 32 from the Mulden Group molasse has no equivalents in the Central Kaoko Zone or the Orogen Core unit of the Kaoko Belt.

Fig. 6 shows the results of the detrital zircon dating from this study and from previous studies (Goscombe et al., 2005; Konopásek et al., 2014) in the medium – high-grade part of the Kaoko Belt pooled into three groups. These groups represent: a) the rifting-related sedimentation with the source region represented by the Congo Craton ± temporal equivalent of the Namaqua Natal Complex/Rehoboth Inlier (Fig. 6a), b) sedimentation with the source in the Punta del Este–Coastal Terrane (Fig. 6b) and c) the late-orogenic molasse sediments of the Mulden Group (Fig. 6c).

3. Comparison with the U–Pb zircon provenance data from the Damara and Gariep belts

Basei et al. (2005), Zimmermann et al. (2011) and Hofmann et al (2014; 2015) presented detrital zircon data from the pre-collisional clastic metasedimentary rocks of the Gariep Belt. The pre-Marinoan continental rift deposits of the par-autochthonous Port Nolloth Zone show one broad peak of detrital zircon dates between *ca.* 1.00 and 1.40 Ga and another group of data between *ca.* 1.75 and 2.10 Ga. This pattern matches with that observed in our samples NL 20 and NL 24B. However, the detrital zircon data obtained directly from the Marinoan Witputs diamictite by Zimmermann et al. (2011) and Hofmann et al. (2015) show the same distribution of dates as the pre-Marionan sediments suggesting that the present day western edge of the Kalahari Craton was at that time still receiving the detrital material from the underlying basement.

The detrital zircon ages obtained from the upper part of the clastic sedimentary sequence in the allochthonous Marmora Terrane of the Gariep Belt show matching pattern with our samples from the top of the studied profile in the Central Kaoko Zone (our samples NL 27, HKB-1, MDB-5 and NL 29), i.e. one group of data between *ca.* 600 and 700 Ma,

another group between *ca.* 900 Ma and 1.05 Ga and some data close to 1.80–1.90 Ga (Basei et al., 2005).

Foster et al. (2015) published a dataset of detrital zircon dates for various stratigraphic units of the Damara Belt. Their samples from the basal Nosib Group overlying the Congo Craton basement in the Central Zone of the Damara Belt show one maximum at *ca.* 1.00 Ga and some data at *ca.* 2.00 Ga. Although stratigraphically older, their sample from the Nosib Group, just like our samples NL 21, NL 25, NL 26 and MDB-6, suggests availability of a local source with rocks representing only one or two age groups. Samples of Foster et al. (2015) collected below or within the Marinoan (*ca.* 635 Ma) Naos diamictite along the northern edge of the Kalahari Craton show very good correlation of the detrital zircon age patterns with our samples NL 20 and NL 24B. The data cover almost the entire interval between *ca.* 1.00 and 2.00 Ga, in case of the data by Foster et al. (2015) showing one broad peak centred at *ca.* 1.20 Ga and another at *ca.* 1.85 Ga (only data for their samples DF09-4 and DF 09-12a).

Most striking is the match of the detrital zircon data of Foster et al. (2015) from the Karibib and Kuiseb formations of the Damara Belt with the data from the uppermost sedimentary succession in the Central Kaoko Zone and the Orogen Core unit in the Kaoko Belt (samples NL 27, HKB-1, MDB-5 and NL 29 in this study and NH 059, NL 15 and NI 133 in Konopásek et al., 2014). The same match is also seen with the sample of Basei et al. (2005) from the sediments of the Marmora Terrane in the Gariep Belt. Even though each of the above-mentioned samples shows variable proportion of zircon grains older than *ca.* 1.30 Ga, they always show one peak at *ca.* 1.00 – 1.10 Ga in a group of data between *ca.* 950 Ma and 1.20 Ga, and one or two peaks in a group of dates between *ca.* 600 and 900 Ma. The youngest peak in the latter group of dates is usually centred at *ca.* 650 Ma and the other peaks appear anywhere between *ca.* 700 and 800 Ma (Fig. 5). This similarity suggests that the

uppermost parts of the Congo Craton cover in the Central Kaoko Zone and the Orogen Core unit of the Kaoko Belt has the same source of the detrital material as the Karibib and Kuiseb formations of the Central and Southern zones of the Damara Belt (the Swakop and Khomas zones, respectively, of Hoffmann et al., 2004). Moreover, the presence of the *ca.* 635 Ma Ghaub Formation diamictite in the uppermost greywacke horizon of the sampled profile in the eastern Central Kaoko Zone shows that these greywackes are temporally equivalent to the uppermost Okonguarri/Arandis and the lowermost Karibib formations in the Damara Belt (see summary of the Damara Belt stratigraphy by Hoffmann et al., 2004).

4. The meaning of the ca. 800–650 Ma detrital zircon populations in the metasediments of the Kaoko, Damara and Gariep belts

As discussed above, the presence of a large proportion of the *ca.* 650 Ma detrital zircon together with detrital zircon with ages between *ca.* 800 and 770 Ma is critical for the provenance of the clastic lower part of the Karibib Formation and the Kuiseb Formation in the Damara Belt, and their temporal equivalents in the Kaoko and Gariep belts. This clastic sedimentation preceded the deposition of the late orogenic molasse (the Mulden Group in northern Namibia and the Nama Group in the south) in the Kaoko, Damara and Gariep belts and, according to the position in the profile studied in this work, started shortly before the time of the *ca.* 645–635 Ma Marinoan glaciation. As discussed above, the closest tectonic unit containing the 650 Ma felsic igneous or metamorphic rocks together with older Neoproterozoic (*ca.* 800–770 Ma) zircon-bearing (meta)igneous rocks is the Punta del Este–Coastal Terrane (Seth et al., 1998; S. Kröner et al., 2004; Konopásek et al., 2008; Gross et al., 2009; Oyhantçabal et al., 2009; Lenz et al., 2011). Because the Karibib/Kuiseb formations-equivalent sedimentary rocks were already involved in the Kaoko Belt orogenesis, the Punta

del Este–Coastal Terrane must have been uplifted prior to its thrusting over the attenuated Congo Craton margin that took place at *ca.* 580–550 Ma (Goscombe et al., 2005; Ulrich et al., 2010; Konopásek et al., 2014) and provide the detrital material for the sedimentation. This uplift is well documented on the South American side of the Kaoko–Dom Feliciano–Gariep orogenic system, where the cooling related to the exhumation of the Punta del Este Terrane has been determined at *ca.* 620–625 Ma (K–Ar white mica cooling ages; Oyhantçabal et al., 2009). All these data suggest that the clastic sedimentary rocks of the Karibib and Kuiseb formations, as well as their temporal equivalents in the Kaoko and Gariep belts represent early orogenic flysch sediments of the Kaoko–Dom Feliciano–Gariep orogenic system related to the compressional tectonics and associated uplift along its western edge in the Dom Feliciano Belt. The position of the samples in which the detrital zircon data suggest their affinity to the early orogenic flysch is shown in Fig. 7. The distribution of the samples suggests a regional character of the early flysch sedimentation and the only position, in which the flysch is apparently missing is the pre-collisional (par)authochthon along the western edge of the Kalahari Craton (see data in Hofmann et al., 2014; 2015).

5. Implications for a pre-convergence configuration of tectonic units in the Kaoko–Dom Feliciano–Gariep orogenic system

Recognition of the Punta del Este–Coastal Terrane as the source of the detrital material for the clastic sediments of the Karibib and Kuiseb formations and their temporal equivalents in the Kaoko and Gariep belts is critical for the understanding of the pre-convergence position of the tectonic units in the Kaoko–Dom Feliciano–Gariep and Damara belts. Clastic sediments at the bottom of the Karibib formation in the Damara Belt appear directly above the *ca.* 635 Ma Ghaub Formation diamictite without the presence of any erosional unconformity, so

according to the stratigraphy of the Damara Belt revised by Hoffmann et al. (2004) is their age *ca.* 630 Ma. The sedimentary age of the samples NL 27, HKB-1, MDB-5 and NL 29 from the uppermost strata of the Congo Craton cover in the easternmost Central Kaoko Zone is very similar, given the presence of the glaciogenic horizon recognized as the Ghaub Formation diamictite. This fact shows that the Punta del Este–Coastal Terrane started to be uplifted and provide sediments for the cover of the Congo Craton already during or shortly after its high-grade metamorphism at 650–630 Ma, i.e. 50–80 myr prior to its thrusting over the attenuated Congo margin in the Kaoko Belt. This timing provides an evidence for the pre-convergence proximity of these two units first suggested by Goscombe and Gray (2007; 2008) and recently discussed by Konopásek et al. (2014). The proximity of the Coastal Terrane as the source region and the Congo Craton margin as the deposition region at *ca.* 635–630 Ma shows that the Coastal Terrane was situated at the attenuated cratonic margin already at the time of its high-grade metamorphism at *ca.* 650–630 Ma. The fact that there is no evidence for any convergent movements in the Kaoko Belt prior this period allows us to draw the conclusion that the Coastal Terrane has been already during the Neoproterozoic rifting an integral part of the rifted Congo Craton margin. These two units were never separated by an oceanic domain that could have been subducted during the late Neoproterozoic evolution of the Kaoko Belt. Such conclusion is in agreement with the pre-collisional position of the Coastal Terrane inferred by Goscombe and Gray (2007), as well as with the assumed evolution of the Gariep Belt (Basei et al., 2005; Frimmel et al., 2011) representing the southeastern part of the same orogenic system.

However, all those models assume that the eastern edge of the Kaoko–Dom Feliciano–Gariep orogenic system represents a back-arc domain developed above a subducting oceanic domain (Adamastor or Brazilides Ocean) that opened approximately between 720 and 650 Ma. Konopásek et al. (2014) dated the youngest syn-rifting igneous rocks in the Kaoko Belt at

ca. 710 Ma. Based on sedimentological data from the Otavi Platform, Hoffman and Halverson (2008) inferred that the rift–drift transition took place between the deposition of the glaciogenic sediments of the Chuos (Sturtian in age) and the Ghaub (Marinoan in age) formations and suggested its timing at *ca.* 680 Ma. However, this time constraint does not fit with the recent estimates for the termination of the Sturtian glaciation, which place it at *ca.* 660 Ma (Rooney et al., 2011; 2015). This, together with the uplift of the Punta del Este–Coastal Terrane, its erosion and deposition of the early flysch sediments in the Kaoko Belt already before *ca.* 635 Ma constrains the maximum lifetime of a hypothetical oceanic domain (Adamastor or Brazilides Ocean) between the eastern and western forelands of the Kaoko–Dom Feliciano–Gariep orogenic system to less than 25 myr. With such time available for opening and closure, the oceanic domain could have reached a large width (> 1000 km) only at extreme spreading rates observed at present e.g. along the East Pacific Rise (e.g. Müller et al., 2008).

Conclusions

The U–Pb zircon provenance study of the Neoproterozoic sedimentary succession covering the Congo Craton in NW Namibia makes it possible to draw the following conclusions:

1) The clastic material for the lower part of the succession was derived from a source that contained both the Paleo- and Mesoproterozoic units. The origin of such detritus is interpreted as a result of erosion of the Paleoproterozoic (meta)igneous rocks of the Congo Craton basement with volcanosedimentary cover or intrusions of Mesoproterozoic age.

2) Clastic metasedimentary rocks in the middle part of the succession including the Sturtian diamictite of the Chuos Formation show the dominance of the Paleoproterozoic detrital zircon, whereas the proportion of Mesoproterozoic zircon grains is small. This is consistent

with the interpretation that at the time of the sedimentation, the Mesoproterozoic volcanosedimentary cover was already eroded away and the dominant source was the Congo Craton basement.

3) The clastic sedimentation in the lower and middle part of the succession is attributed to the early Neoproterozoic rifting period.

4) The uppermost part of the succession contains predominantly late-Mesoproterozoic and Neoproterozoic detrital zircon populations that point to the Punta del Este–Coastal Terrane in the centre of the Kaoko–Dom Feliciano–Gariep orogen as a source region. The presence of the Marinoan (*ca.* 645–635 Ma) glaciogenic interval within the metasediments dates the onset of early foredeep sedimentation at *ca*. 650–645 Ma.

5) The erosion of the Punta del Este–Coastal Terrane in the west, and the dispersal of the sediment towards the eastern foreland of the orogen suggest that the uppermost strata of the studied profile represent an early orogenic flysch that was later involved into collisional processes forming the Kaoko Belt. The early flysch sediments can be traced also in the Damara and Gariep belts, which suggests their regional character.

6) The dispersal of the early flysch sediments sourced in the Punta del Este–Coastal Terrane on top of the western edge of the Congo Craton already at ca. 650–645 Ma, as well as the *ca.* 50–80 myr time span between its sedimentation and the thrusting of the Coastal Terrane over the Congo Craton margin is evidence that these two crustal domain were never separated by an oceanic domain. On the contrary, before its thrusting over the Congo Craton margin, the Coastal Terrane was an integral part of it and represented a part of the rift system. Such conclusion is in accord with existing models for the tectonic evolution of the Kaoko–Dom Feliciano–Gariep orogenic system (e.g. Basei et al., 2005; Goscombe and Gray, 2007; Frimmel et al., 2011)

7) The time difference between the estimates for the end of active crustal stretching and the onset of convergence marking the beginning of the development of the Kaoko–Dom Feliciano–Gariep orogen is less than 25 myr. With this time available for an opening and closure, a potential oceanic domain developed after the rifting period must have been narrow. Such a short timespan between the break-up and onset of collision poses a problem for models implying that the convergent tectonic evolution of the Kaoko–Dom Feliciano–Gariep orogen was driven by subduction of the Adamastor/Brazilides Ocean.

Acknowledgement

The work was financially supported by the Czech Science Foundation (15-05988S). The authors appreciate logistic support of the Geological Survey of Namibia. The article benefited from careful reviews of Hartwig Frimmel and one anonymous reviewer.

Appendix A. – Analytical techniques

Zircon separation techniques

Approximately 3 to 5 kg of rock material for each sample was crushed and disintegrated using disc mill to obtain grain fraction between *ca.* 50–500 microns in size. The milled samples were sieved to obtain the size fraction <315 microns and this fraction was processed by using the Wilfley table in order to concentrate the heavy minerals. The heavy fraction of the samples was loaded to sodium polytungstate (SPT) and subsequently to diiodomethane (DIM) heavy liquids, followed by removal of the magnetic minerals from the heavy fraction using the Frantz isodynamic separator. Zircon crystals were then transferred in ethanol from the pool of separated grains to a double-sided tape using pipette and mounted in 1 inch epoxy-filled blocks and polished using SiC and diamond paste to obtain even surfaces suitable for cathodoluminescence imaging and laser ablation ICP-MS analysis.

Zircon imaging and LA-ICP-MS techniques

Cathodoluminescence images of zircon were obtained using the Zeiss Supra 55 VP scanning electron microscope at the University of Bergen. Prior to U–Pb analysis, the carbon coating was removed and the sample surfaces were cleaned with 2% HNO_3, DI water, and ethanol.

Isotopic analysis of zircon in samples labelled NL and NM followed the technique described in Košler et al. (2002). A Thermo-Finnigan Element 2 sector field ICP-MS coupled to a 193 ArF Excimer laser (Resonetics RESOlution M50-LR) at Bergen University was used to measure Pb/U and Pb isotopic ratios in zircon grains. The sample introduction system was modified to enable simultaneous nebulisation of a tracer solution and laser ablation of the solid sample (Horn et al., 2000). Natural Tl ($^{205}Tl/^{203}Tl$ = 2.3871 – Dunstan et al., 1980), ^{209}Bi and enriched ^{233}U and ^{237}Np (>99%) were used in the tracer solution, which was aspirated to the plasma in an argon–helium carrier gas mixture through an Apex desolvation nebuliser (Elemental Scientific) and a T-piece tube attached to the back end of the plasma torch. A helium gas line carrying the sample from the laser cell to the plasma was also attached to the T-piece tube. The laser was set up to produce energy density of ca 7 J/cm^2 at a repetition rate of 5 Hz. The laser beam was imaged on the surface of the sample placed in the two-volume ablation cell, which was mounted on a computer-driven motorised stage of a microscope. During ablation the stage was moved beneath the stationary laser beam (19–26 μm in diameter) to produce a linear raster in the sample. Typical acquisitions consisted of a 35 second measurement of analytes in the gas blank and aspirated solution, particularly ^{203}Tl – ^{205}Tl – ^{209}Bi – ^{233}U – ^{237}Np, followed by measurement of U and Pb signals from zircon, along with the continuous signal from the aspirated solution, for another 120 seconds. The data were acquired in time resolved – peak jumping – pulse counting mode with 1 point measured per peak for masses 202 (flyback), 203 and 205 (Tl), 206 and 207 (Pb), 209 (Bi), 233 (U), 237

(Np), 238 (U), 249 (233U oxide), 253 (237Np oxide) and 254 (238U oxide). Raw data were corrected for dead time of the electron multiplier and processed off line in a spreadsheet-based program Lamdate (Košler et al., 2002). Data reduction included correction for gas blank, laser-induced elemental fractionation of Pb and U and instrument mass bias. Minor formation of oxides of U and Np was corrected for by adding signal intensities at masses 249, 253 and 254 to the intensities at masses 233, 237 and 238, respectively. No common Pb correction was applied to the data. Details of data reduction and corrections are described in Košler et al. (2002) and Košler and Sylvester (2003). Zircon reference material 91500 (1065 Ma – Wiedenbeck et al., 1995) and GJ-1 (609 Ma – Jackson et al., 2004) were periodically analysed during this study and they yielded pooled concordia ages of 1065 ± 3 and 608 ± 2 Ma, respectively.

A Nu AttoM high resolution ICP-MS was used to measure the Pb/U and Pb isotopic ratios in zircon crystals extracted from samples labelled HKB and MDB. The laser was fired at a repetition rate of 5 Hz and energy of 80 mJ with 19 microns spot size. Typical acquisitions consisted of 15 second measurement of blank followed by measurement of U and Pb signals from the ablated zircon for another 30 seconds. The data were acquired in time resolved – peak jumping – pulse counting mode with 1 point measured per peak for masses ^{204}Pb + Hg, ^{206}Pb, ^{207}Pb, ^{208}Pb, ^{232}Th, ^{235}U, and ^{238}U. Due to a non-linear transition between the counting and attenuated (= analog) acquisition modes of the ICP instruments, the raw data were pre-processed using a purpose-made Excel macro. As a result, the intensities of ^{238}U are left unchanged if measured in a counting mode and recalculated from ^{235}U intensities if the ^{238}U was acquired in an attenuated mode. Data reduction was then carried out off-line using the Iolite data reduction package version 3.0 with VizualAge utility (Petrus and Kamber, 2012). Full details of the data reduction methodology can be found in Paton et al. (2010). The data reduction included correction for gas blank, laser-induced elemental fractionation of Pb

and U and instrument mass bias. For the data presented here, blank intensities and instrumental bias were interpolated using an automatic spline function while down-hole inter-element fractionation was corrected using an exponential function. No common Pb correction was applied to the data but the low concentrations of common Pb was controlled by observing $^{206}Pb/^{204}Pb$ ratio during measurements. Residual elemental fractionation and instrumental mass bias were corrected by normalization to the natural zircon reference material 91500 (Wiedenbeck et al., 1995). Zircon reference materials Plešovice (Sláma et al., 2008) and GJ-1 (Jackson et al., 2004) were periodically analysed during the measurement for quality control and the obtained mean values of 334 ± 3 (2σ) Ma and 610 ± 3 (2σ) Ma are 1% accurate within the published reference values (337 Ma, Sláma et al., 2008; 609 Ma Jackson et al., 2004, respectively).

Whole rock Nd isotopic analysis

For the radiogenic isotope determinations, the samples were dissolved using a combined HF–HCl–HNO_3 acid attack. Strontium and neodymium from samples marked NL were isolated by exchange chromatography techniques following a chemical separation described by Le Roex and Lanyon (1998). Sm–Nd isotopic analyses were performed on a Finnigan MAT 262 thermal ionization mass spectrometer housed at the University of Bergen in dynamic ($^{143}Nd/^{144}Nd$) and static ($^{148}Nd/^{144}Nd$ and $^{149}Sm/^{152}Sm$) mode using a double Re filament assembly. Concentrations of Nd and Sm were quantified by isotopic dilution with in-house ^{148}Nd-^{149}Sm mixed spike. The $^{143}Nd/^{144}Nd$ ratios were corrected for mass fractionation to $^{146}Nd/^{144}Nd = 0.7219$ (Wasserburg et al., 1981). External reproducibility was estimated from repeat analyses of the La Jolla ($^{143}Nd/^{144}Nd = 0.511850 \pm 0.000006$, 2σ) isotopic standard.

Strontium and neodymium in samples marked MDB and HKB were isolated from bulk matrix by the column chromatography techniques using TRU, Ln and Sr resins (Triskem Intl.) by method adapted from Pin et al. (1994) and Pin and Zalduegui (1997). Isotopic analyses were performed on a MC-ICP-MS Neptune (Thermo-Fisher Scientific) housed at the Czech Geological Survey in Prague. The $^{143}Nd/^{144}Nd$ ratios were corrected for mass fractionation to $^{146}Nd/^{144}Nd = 0.7219$ (Wasserburg et al., 1981). External reproducibility was estimated from repeat analyses of the JNdi-1 ($^{143}Nd/^{144}Nd = 0.512081 \pm 15$ (2σ, n = 20)) isotopic standard. Results were recalculated to recommended JNdi-1 value of $^{143}Nd/^{144}Nd = 0.512115$ (Tanaka et al., 2000). The Sm and Nd concentrations were obtained by Q-ICP-MS.

The decay constants applied to age-correct the isotopic ratios are from Lugmair and Marti (1978). The ε_{Nd} values were obtained using Bulk Earth parameters of Jacobsen and Wasserburg (1980), the two-stage Depleted Mantle Nd model ages (T^{Nd}_{DM}) were calculated after Liew and Hofmann (1988).

Appendix B. (Electronic) – Supplementary data

Data_HKB-1.xls

Data_MDB-5.xls

Data_MDB-6.xls

Data_NL20.xls

Data_NL21.xls

Data_NL24B.xls

Data_NL25.xls

Data_NL26.xls

Data_NL27.xls

Data_NL29.xls

Data_NM32.xls

REFERENCES

Basei, M.A.S., Frimmel, H.E., Nutman, A.P., Preciozzi, F., Jacob, J., 2005. A connection between the Neoproterozoic Dom Feliciano (Brazil/Uruguay) and Gariep (Namibia/South Africa) orogenic belts – evidence from a reconnaissance provenance study. Precambrian Res. 139, 195–221.

Basei, M.A.S., Peel, E., Bettuci, L.S., Preciozzi, F., Nutman, A.P., 2011. The basement of the Punta del Este Terrane (Uruguay): an African Mesoproterozoic fragment at the eastern border of the South American Río de La Plata craton. Int. J. Earth Sci. 100, 289–304.

Basei, M.A.S., Siga Jr., O., Masquelin, H., Harara, O.M., Reis Neto, J.M., Preciozzi, F., 2000. The Dom Feliciano Belt (Brazil–Uruguay) and its foreland (Rio de la Plata Craton): Framework, tectonic evolution and correlations with similar terranes of southwestern Africa. In: Cordani, U.G., Milani, E.J., Thomaz Filho, A., Campos, D.A. (Eds.), Tectonic Evolution of South America. Rio de Janeiro, 311–334.

Becker, T., Schreiber, U., Kampunzu, A.B., Armstrong, R., 2006. Mesoproterozoic rocks of Namibia and their plate tectonic setting. J. Afr. Earth Sci. 46, 112–140.

Cawood, P.A., Strachan, R.A., Pisarevski, S.A., Gladkochub, D.P., Murphy, J.B., 2016. Linking collisional and accretionary orogens during Rodinia assembly and breakup: Implications for models of supercontinent cycles. Earth Planet. Sci. Lett. 449, 118–126.

Chemale Jr., F., Mallmann, G., Bitencourt, M.F., Kawashita, K., 2012. Time constraints on magmatism along the Major Gercino Shear Zone, southern Brazil: Implications for West Gongwana reconstruction. Gondwana Res. 22, 184–199.

Condon, D., Zhu, M., Bowring, S., Wang, W., Yang, A., Jin, Y., 2005. U–Pb ages from the Neoproterozoic Doushantuo Formation, China. Science 308, 95–98.

Dingeldey, D.P., Dürr, S.B., Charlesworth, E.G., Franz, L., Okrusch,M., Stanistreet, I.G., 1994. A geotraverse through the northern coastal branch of the Damaran orogen west of Sesfontein, Namibia. J. Afr. Earth Sci. 19, 315–329.

Dunstan, L.P., Gramch, J.W., Barnes, I.L., Purdy, W.C., 1980. The absolute abundance and the atomic weight of a reference sample of thallium. J. Res. Nat. Bur. Stand. 85, 1–10.

Foster, D.A., Goscombe, B.D., Newstead, B., Mapani, B., Mueller, P.A., Gregory, L.C., Muvangua, E., 2015. U–Pb age and Lu–Hf isotopic data of detrital zircons from the Neoproterozoic Damara Sequence: Implications for Congo and Kalahari before Gondwana. Gondwana Res. 28, 179–190.

Franz, L., Romer, R.L., Dingeldey, D.P., 1999. Diachronous Pan-African granulite-facies metamorphism (650 Ma and 550 Ma) in the Kaoko belt, NW Namibia. Eur. J. Mineral. 11, 167–180.

Frimmel, H.E., Basei, M.S., Gaucher, C., 2011. Neoproterozoic geodynamic evolution of SW-Gondwana: a southern African perspective. Int. J. Earth Sci. 100, 323–354.

Goscombe, B.D., 1998a. Geological map of Tomakas 1:50,000 sheet. Geol. Surv. Namibia.

Goscombe, B.D., 1998b. Geological map of Omapungwe 1:50,000 sheet. Geol. Surv. Namibia.

Goscombe, B., Gray, D.R., 2007. The Coastal Terrane of the Kaoko Belt, Namibia: Outboard arc-terrane and tectonic significance. Precambrian Res. 155, 139–158.

Goscombe, B., Gray, D., Armstrong, R., Foster, D.A., Vogl, J., 2005. Event geochronology of the Pan-African Kaoko Belt, Namibia. Precambrian Res. 140, 103.e1–103.e41.

Goscombe, B., Hand, M., Gray, D., Mawby, J., 2003. The metamorphic architecture of a transpressional orogeny: the Kaoko Belt, Namibia. J. Petrol. 44, 679–711.

Gray, D.R., Foster, D.A., Meert, J.G., Goscombe, B.D., Armstrong, R., Trouw, R.A.J., Passchier, C.W., 2008. A Damara Orogen perspective on the assembly of southwestern Gondwana. In: Pankhurst, R.J., Trouw, R.A.J., de Brito Neves, B.B., de Wit, M.J. (Eds.), West Gondwana: Pre-Cenozoic correlations across the south Atlantic region. Geol. Soc. London Spec. Pub. 294, 257–278.

Gross, A.O.M.S., Droop, G.T.R., Porcher, C.C., Fernandes, L.A.D., 2009. Petrology and thermobarometry of mafic granulites and migmatites from the Chafalote Metamorphic Suite: New insights into the Neoproterozoic P-T evolution of the Uruguayan–Sul-Rio-Grandense shield. Precambrian Res. 170, 157–174.

Guj, P., 1970. The Damara mobile belt in the south-western Kaokoveld, SouthWest Africa. University of Cape Town Precambrian Research Unit Bulletin, 10 (168 pp.).

Halverson, G.P., Hoffman, P.F., Schrag, D.P., Maloof, A.C., Rice, A.H.N., 2005. Toward a Neoproterozoic composite carbon-isotope record. Geol. Soc. Am. Bull. 117,1181–1207.

Hartnady, C., Joubert, P., Stowe, C., 1985. Proterozoic crustal evolution in southwestern Africa. Episodes 8, 236–244.

Heine, C., Zoethout, J., Müller, R.D., 2013. Kinematics of the South African rift. Sol. Earth 4, 215–253.

Hoffmann, K.-H., Condon, D.J., Bowring, S.A., Crowley, J.L., 2004. U–Pb zircon date from the Neoproterozoic Ghaub Formation,Namibia: constraints on Marinoan glaciation. Geology 32, 817–820.

Hoffmann, K.-H., Prave, A.R., 1996. A preliminary note on a revised subdivision and regional correlation of the Otavi Group based on glaciogenic diamictites and associated cap dolostones. Comm. Geol. Surv. Namibia 11, 77–82.

Hoffman, P.F., Halverson, G.P., 2008. Otavi Group of the western Northern Platform, the Eastern Kaoko Zone and the western Northern Margin Zone. In: Miller, R. McG. (Ed.) The Geology of Namibia, vol. 2. Geol. Surv. Namibia, Windhoek, pp. 13-69–13-136.

Hoffman, P.F., Hawkins, D.P., Isachen, C.E., Bowring, S.A., 1996. Precise U–Pb zircon ages for early Damaran magmatism in the Summas Mountains and Welwitschia Inlier, northern Damara belt, Namibia. Communications of the Geological Survey of Namibia 11, 47–52.

Hofmann, M., Linnemann, U., Hoffmann, K.-H., Gerdes, A., Eckelmann, K., Gärtner, A., 2014. The Namuskluft and Dreigratberg sections in southern Namibia (Kalahari Craton, Gariep Belt): a geological history of Neoproterozoic rifting and recycling of cratonic crust during the dispersal of Rodinia until the amalgamation of Gondwana. Int. J. Earth Sci. 103, 1187–1202.

Hofmann, M., Linnemann, U., Hoffmann, K.-H., Germs, G., Gerdes, A., Marko, L., Eckelmann, K., Gärtner, A., Krause, R., 2015. The four Neoproterozoic glaciations of southern Namibia and their detrital zircon record: The fingerprints of four crustal growth events during two supercontinent cycles. Precambrian Res. 259, 176–188.

Horn, I., Rudnick, R.L., McDonough, W.F., 2000. Precise elemental and isotope ratio measurement by simultaneous solution nebulisation and laser ablation-ICP-MS: application to U–Pb geochronology. Chem. Geol. 164, 281–301.

Jackson, S.E., Pearson, N.J., Griffin, W.L., Belousova, E.A., 2004. The application of laser ablation-inductively coupled plasma-mass spectrometry to in situ U–Pb zircon geochronology. Chem. Geol. 211, 47–69.

Jacobsen, S.B., Wasserburg, G.J., 1980. Sm–Nd isotopic evolution of chondrites. Earth Planet. Sci. Lett. 50, 139–155.

Janoušek, V., Konopásek, J., Ulrich, S., Erban, V., Tajčmanová, L., Jeřábek, P., 2010. Geochemical character and petrogenesis of Pan-African Amspoort suite of the Boundary Igneous Complex in the Kaoko Belt (NW Namibia). Gondwana Res. 18, 688–707.

Jung, S., Kröner, A., Kröner, S., 2007. A 700 Ma Sm–Nd garnet–whole rock age from the granulite facies Central Kaoko Zone (Namibia): evidence for a cryptic high-grade polymetamorphic history? Lithos 97, 247–270.

Kleinhanns, I.C., Fullgraf, T., Wilsky, F., Nolte, N., Fliegel, D., Klemd, R., Hansen, B.T., 2015. U–Pb zircon ages and (isotope) geochemical signatures of the Kamanjab Inlier (NW Namibia): constraints on Palaeoproterozoic crustal evolution along the southern Congo Craton. In: Roberts, N.M.W., Van Kranendonk, M., Parman, S., Shirey, S., Clift, P.D. (Eds.), Continent formation through time. Geol. Soc. London Spec. Pub. 389, 165–195.

Konopásek, J., Košler, J., Sláma, J., Janoušek, V., 2014. Timing and sources of pre-collisional Neoproterozoic sedimentation along the SW margin of the Congo Craton (Kaoko Belt, NW Namibia). Gondwana Res. 26, 386–401.

Konopásek, J., Košler, J., Tajčmanová, L., Ulrich, S., Kitt, S.L., 2008. Neoproterozoic igneous complex emplaced along major tectonic boundary in the Kaoko Belt (NW Namibia): ion probe and LA-ICP-MS dating of magmatic and metamorphic zircons. J. Geol. Soc. London 165, 153–165.

Konopásek, J., Sláma, J., Košler, J., 2016. Linking the basement geology along the Africa-South America coasts in the South Atlantic. Precambrian Res. 280, 221–230.

Košler, J., Fonneland, H., Sylvester, P., Tubrett, M., Pedersen, R.B., 2002. U–Pb dating of detrital zircons for sediment provenance studies— a comparison of laser ablation ICPMS and SIMS techniques. Chem. Geol. 182, 605–618.

Košler, J., Sylvester, P., 2003. Present trends and the future of zircon in geochronology: laser ablation ICPMS. In: Hanchar, J.M., Hoskin, P.W.O. (Eds.), Zircon. Reviews in Mineralogy and Geochemistry 53, pp. 243–275.

Kröner, A., Rojas-Agramonte, Y., Hegner, E., Hoffmann, K.-H., Wingate, M.T.D., 2010. SHRIMP zircon dating and Nd isotopic systematics of Palaeoproterozoic migmatitic orthogneisses in the Epupa Metamorphic Complex of northwestern Namibia. Precambrian Res. 183, 50–69.

Kröner, A., Rojas-Agramonte, Y., Wong, J., Wilde, S.A., 2015. Zircon reconnaissance dating of Proterozoic gneisses along the Kunene River of northwestern Namibia. Tectonophysics 662, 125–139.

Kröner, S., Konopásek, J., Kröner, A., Passchier, C.W., Poller, U., Wingate, M.T.D., Hofmann, K.H., 2004. U–Pb and Pb-Pb zircon ages of metamorphic rocks in the Kaoko Belt of Northwestern Namibia: A Palaeo- to Mesoproterozoic basement reworked during the Pan-African orogeny. South Afr. J. Geol. 107, 455–476.

Le Roex, A.P., Lanyon, R., 1998. Isotope and trace element geochemistry of Cretaceous Damaraland lamprophyres and carbonatites, northwestern Namibia: evidence for plume–lithosphere interactions. J. Petrol. 39, 1117–1146.

Lenz, C., Fernandes, L.A.D., McNaughton, N.J., Porcher, C.C., Masquelin, H., 2011. U–Pb SHRIMP ages for the Cerro Bori orthogneisses, Dom Feliciano Belt in Uruguay: Evidences of a ~800 Ma magmatic and ~650 Ma metamorphic event. Precambrian Res. 185, 149–163.

Liew, T.C., Hofmann, A.W., 1988. Precambrian crustal components, plutonic associations, plate environment of the Hercynian Fold Belt of Central Europe: indications from a Nd and Sr isotopic study. Contrib. Mineral. Petrol. 98, 129–138.

Lugmair, G.W., Marti, K., 1978. Lunar initial 143Nd/144Nd: differential evolution line of the lunar crust and mantle. Earth Planet. Sci. Lett. 39, 349–357.

Macdonald, F.A., Schmitz, M.D., Crowley, J.L., Roots, C.F., Jones, D.S., Maloof, A.C., Strauss, J.V., Cohen, P.A., Johnston, D.T., Schrag, D.P., 2010. Calibrating the Cryogenian. Science 237, 1241–1243.

Masberg, P., Mihm, D., Jung, S., 2005. Major and trace element and isotopic (Sr, Nd, O) constraints for Pan-African crustally contaminated grey granite gneisses from the southern Kaoko Belt, Namibia. Lithos 84, 25–50.

Masquelin, H., Fernandes, L.A.D., Lenz, C., Porcher, C.C., McNaughton, N.J., 2012. The Cerro Olivo Complex: a pre-collisional Neoproterozoic magmatic arc in Eastern Uruguay. Int. Geol. Rev. 54, 1161–1183.

Miller, R.M., 1983. The Pan-African Damara Orogen of South West Africa/Namibia. In: Miller, R.M. (Ed.), Evolution of the Damara Orogen of South West Africa/Namibia. Geol. Soc. S. Afr. Spec. Pub. 11, pp. 431–515.

Müller, R.D., Sdrolias, M., Gaina, C., Roest, W.R., 2008. Age, spreading rates, and spreading asymmetry of the world's ocean crust. Geochem. Geophys. Geosyst. 9, Q04006.

Oyhantçabal, P., Siegesmund, S., Wemmer, K., Presnyakov, S., Layer, P., 2009. Geochronological constraints on the evolution of the southern Dom Feliciano Belt (Uruguay). J. Geol. Soc. London 166, 1075–1084.

Passchier, C.W., Trouw, R.A.J., Ribeiro, A., Paciullo, F.V.P., 2002. Tectonic evolution of the southern Kaoko Belt, Namibia. J. Afr. Earth Sci. 35, 61–75.

Paton, C., Woodhead, J.D., Hellstrom, J.C., Hergt, J.M., Greig, A., Maas, R., 2010. Improved laser ablation U–Pb zircon geochronology through robust downhole fractionation correction. Geochem. Geophys. Geosyst. 11, Q0AA06.

Petrus, J.A., Kamber, B.S., 2012. VizualAge: A Novel Approach to Laser Ablation ICP-MS U–Pb Geochronology Data Reduction. Geostand. Geoanal. Res. 36, 247–270.

Pin, C., Briot, D., Bassin, C., Poitrasson, F., 1994. Concomitant Separation of Strontium and Samarium Neodymium for Isotopic Analysis in Silicate Samples, Based on Specific Extraction Chromatography. Anal. Chim. Acta 298, 209–217.

Pin, C., Zalduegui, J.F.S., 1997. Sequential separation of light rare-earth elements, thorium and uranium by miniaturized extraction chromatography: Application to isotopic analyses of silicate rocks. Anal. Chim. Acta 339, 79–89.

Porada, H., 1979. Damara-Ribeira orogeny of the Pan-African-Brasiliano cycle in Namibia (Southwest Africa) and Brazil as interpreted in terms of continental collision. Tectonophysics 57, 237–265.

Porada, H., 1989. Pan-African rifting and orogenesis in southern to equatorial Africa and eastern Brazil. Precambrian Res. 44, 103–136.

Prave, A.R., 1996. Tale of three cratons: Tectonostratigraphic anatomy of the Damara orogen in northwestern Namibia and the assembly of Gondwana. Geology 24, 1115–1118.

Prave, A.R., Condon, D.J., Hoffmann, K.H., Tapster, S., Fallick, A.E., 2016. Duration and nature of the end-Cryogenian (Marinoan) glaciation. Geology 44, 631–634.

Rooney, A.D., Chew, D.M., Selby, D., 2011. Re-Os geochronology of the Neoproterozoic-Cambrian Dalradian Supergroup of Scotland and Ireland: Implications for Neoproterozoic stratigraphy, glaciation and Re-Os systematics. Precambrian Res. 185, 202–214.

Rooney, A.D., Macdonald, F.A., Strauss, J.V., Dudás, F.Ö., Hallmann, C., Selby, D., 2014. Re-Os geochronology and coupled Os-Sr isotope constraints on the Sturtian snowball. Nat. Acad. Sci. Proceed. 111, 51–56.

Rooney, A.D., Strauss, J.V., Brandon, A.D., Macdonald, F.A., 2015. A Cryogenian chronology: Two long-lasting synchronous Neoproterozoic glaciations. Geology 43, 459–462.

Seth, B., Kröner, A., Mezger, K., Nemchin, A.A., Pidgeon, R.T., Okrusch, M., 1998. Archaean to Neoproterozoic magmatic events in the Kaoko belt of NW Namibia and their geodynamic significance. Precambrian Res. 92, 341–363.

Sláma, J., Košler, J., Condon, D.J., Crowley, J.L., Gerdes, A., Hanchar, J.M., Horstwood, M.S.A., Morris, G.A., Nasdala, L., Norberg, N., Schaltegger, U., Schoene, B., Tubrett, M.N., Whitehouse, M.J., 2008. Plešovice zircon - A new natural reference material for U–Pb and Hf isotopic microanalysis. Chem. Geol. 249, 1–35.

Tanaka, T., Togashi, S., Kamioka, H., Amakawa, H., Kagami, H., Hamamoto, T., Yuhara, M., Orihashi, Y., Yoneda, S., Shimizu, H., Kunimaru, T., Takahashi, K., Yanagi, T., Nakano, T., Fujimaki, H., Shinjo, R., Asahara, Y., Tanimizu, M., Dragusanu, C., 2000. JNdi-1: a neodymium isotopic reference in consistency with LaJolla neodymium. Chem. Geol. 168, 279–281.

Ulrich, S., Konopásek, J., Jeřábek, P., Tajčmanová, L., 2011. Transposition of structures in the Neoproterozoic Kaoko Belt (NW Namibia) and their absolute timing. Int. J. Earth Sci. 100, 415–429.

Vermeesch, P., 2012. On the visualisation of detrital age distributions. Chem. Geol. 312, 190–194.

Wasserburg, G., Jacobsen, S., DePaolo, D.J., McCulloch, M., Wen, T., 1981. Precise determination of ratios, Sm and Nd isotopic abundances in standard solutions. Geochim. Cosmochim. Acta 45, 2311–2323.

Wiedenbeck, M., Alle, P., Corfu, F., Griffin, W.L., Meier, M., Oberli, F., Vonquadt, A., Roddick, J.C., Speigel, W., 1995. Three natural zircon standards for U-Th-Pb, Lu-Hf, trace element and REE analyses. Geost. Newsletter 19, 1–23.

Will, T.M., Okrusch, M., Gruner, B.B., 2004. Barrovian and Buchan type metamorphism in the Pan-African Kaoko Belt, Namibia: implications for its geotectonic position within the framework of Western Gondwana. S. Afr. J. Geol. 107, 431–454.

Zimmermann, U., Tait, J., Crowley, Q.G., Pashley, V., Straathof, G., 2011. The Witputs diamictite in southern Namibia and associated rocks: constraints for a global glaciation? Int. J. Earth Sci. 100, 511–526.

FIGURE CAPTIONS

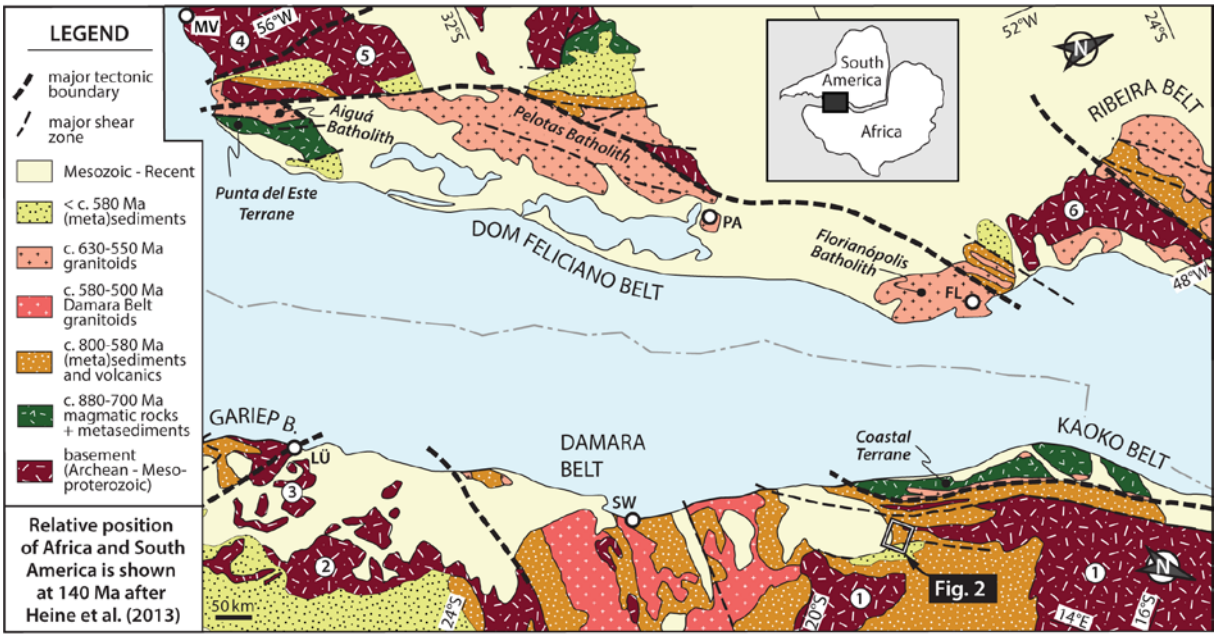

Konopasek et al. - Fig. 1

Figure 1. Simplified geological map of the Dom Feliciano and Kaoko belts (modified after Gross et al., 2009 and Frimmel et al., 2011). The mutual position of Africa and South America is shown at 140 Ma (see inset), the dot-and-dash line shows the inferred position of the rift centre after Heine et al. (2013). Pre-Neoproterozoic domains: 1–Congo Craton; 2-Rehoboth Inlier; 3–Namaqua Metamorphic Complex; 4–Rio de la Plata Craton – Piedra Alta Terrane; 5–Rio de la Plata Craton – Nico Perez Terrane; 6–Luis Alves Terrane. MV–Montevideo; PA–Porto Alegre; FL–Florianópolis; LÜ–Lüderitz; SW–Swakopmund.

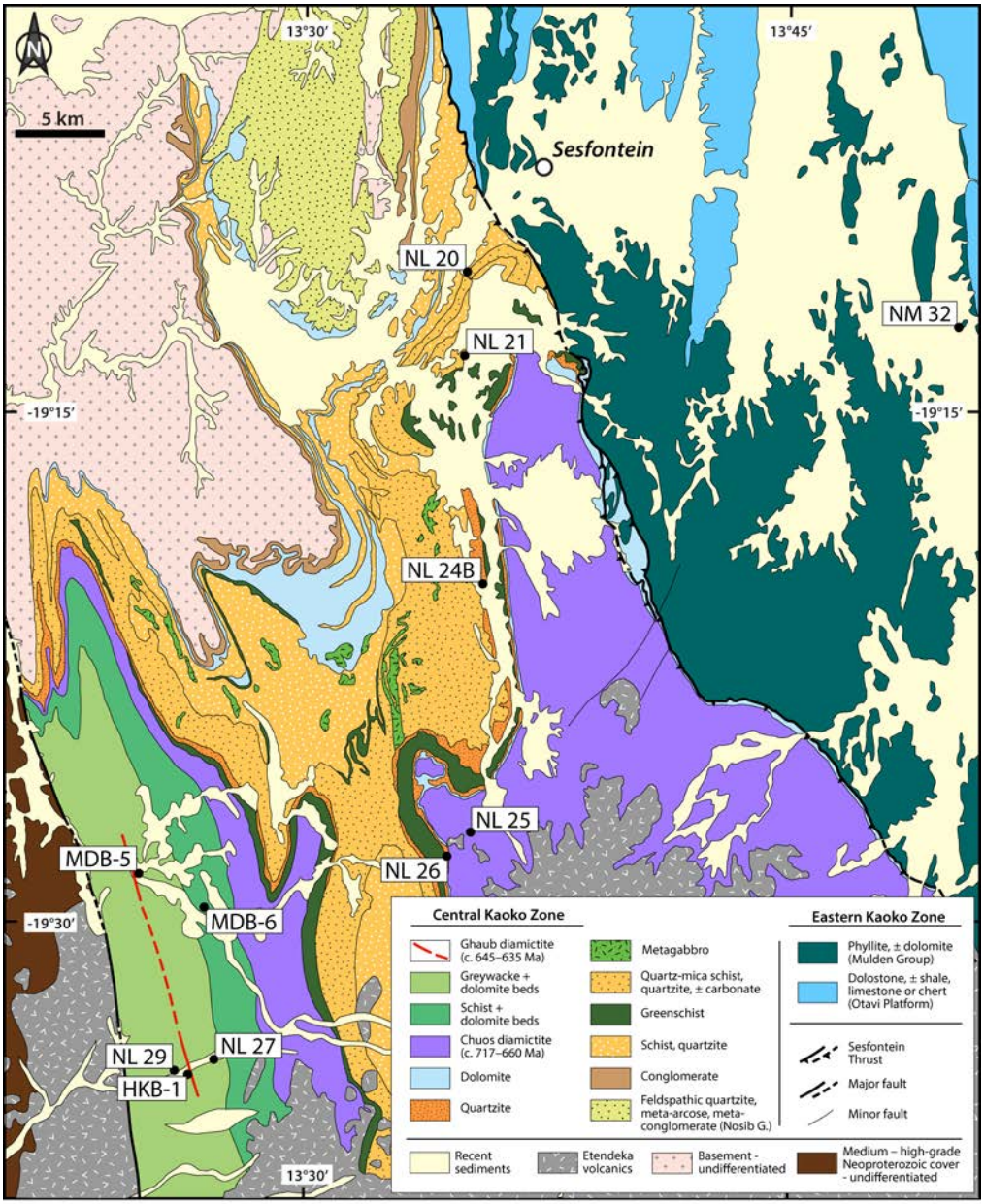

Konopasek et al. - Fig. 2

Figure 2. Geological map of the Sesfontein area in the southeastern part of the Kaoko Belt with the location of the samples used for this study. The map is based mainly on the results of geological mapping by Guj (1970) and it is redrawn from a provisional compilation of the 1:250 000 Geologial Sheet 1912 Sesfontein published by the Geological Survey of Namibia.

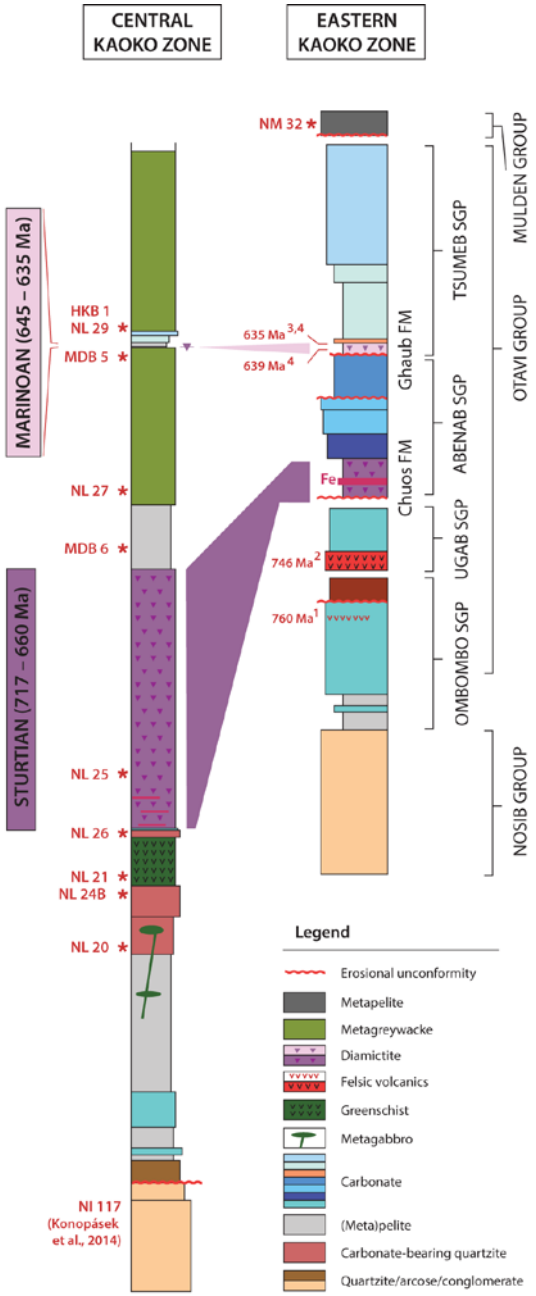

Konopasek et al. - Fig. 3 - single column width

Figure 3. Lithostratigraphic subdivision of the low-grade southeastern part of the Central Kaoko Zone and its correlation with the stratigraphy of the Otavi Group carbonate platform in the Eastern Kaoko Zone. The stratigaphic position of the studied samples is marked by asterisks. Age dates (U-Pb zircon) of volcanic units within the Otavi Group and correlative units of the Swakop Group are from: 1) Halverson et al. (2005), 2) Hoffman et al. (1996), 3) Hoffmann et al. (2004) and 4) Prave et al. (2016).

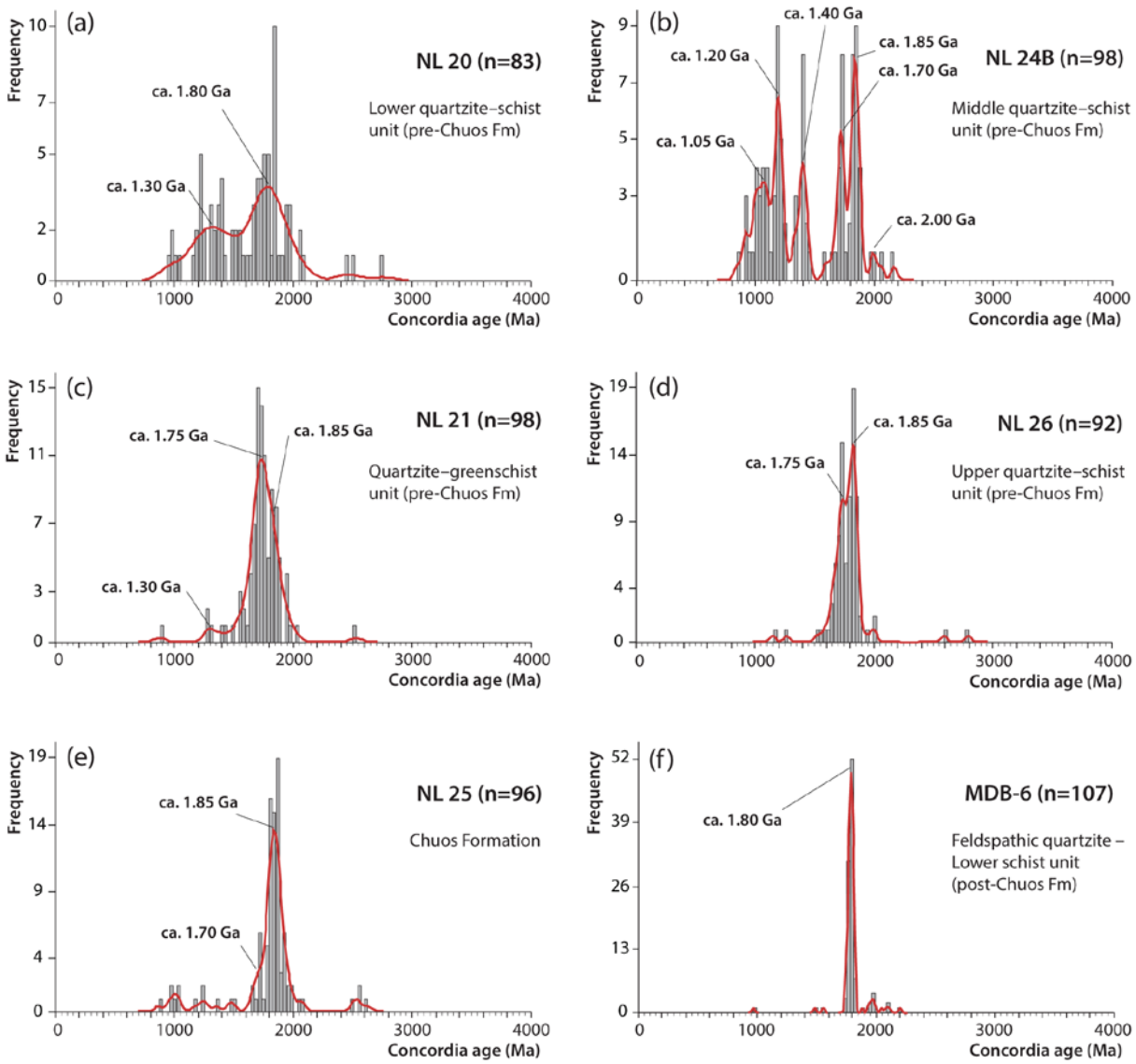

Konopasek et al. - Fig. 4

Figure 4. U–Pb detrital zircon data for the samples of the lower part of the sampled stratigraphic profile. Width of individual bins in the frequency histograms is 30 Ma.

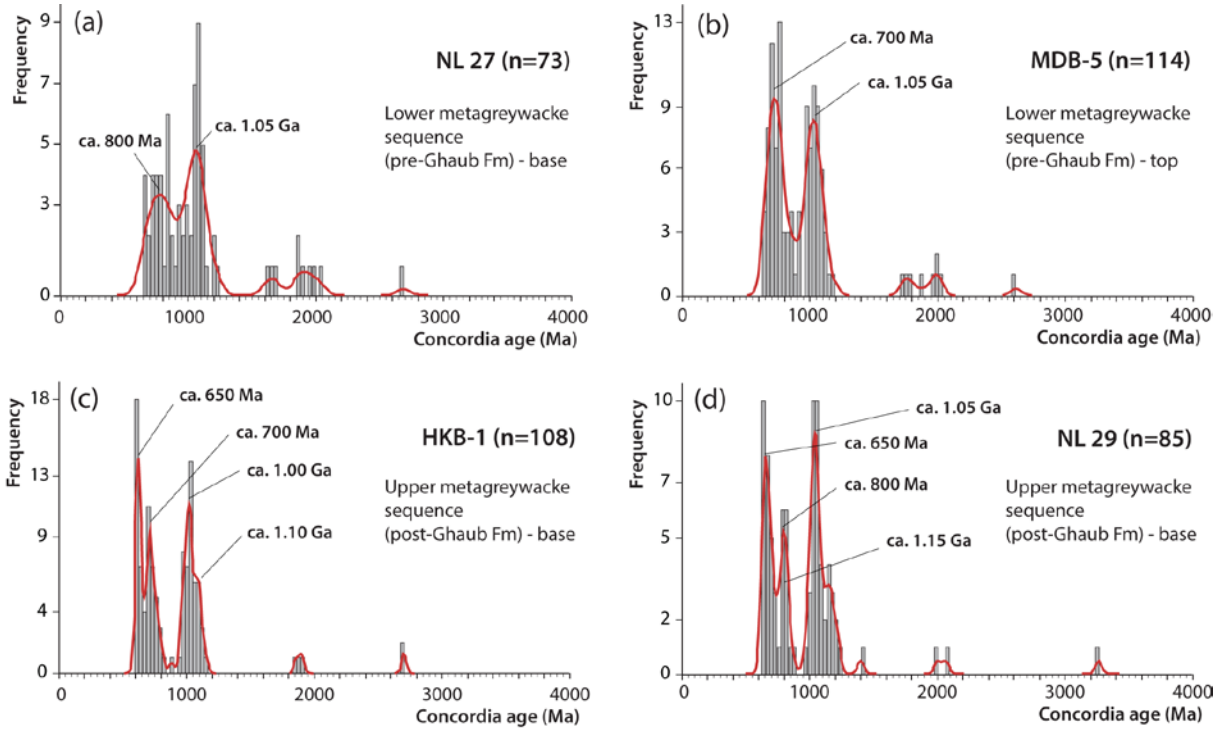

Konopasek et al. - Fig. 5

Figure 5. U–Pb detrital zircon data for the samples of the upper part of the sampled stratigraphic profile in the proximity of the *ca.* 635 Ma glaciogenic horizon of the Ghaub Formation. Width of individual bins in the frequency histograms is 30 Ma.

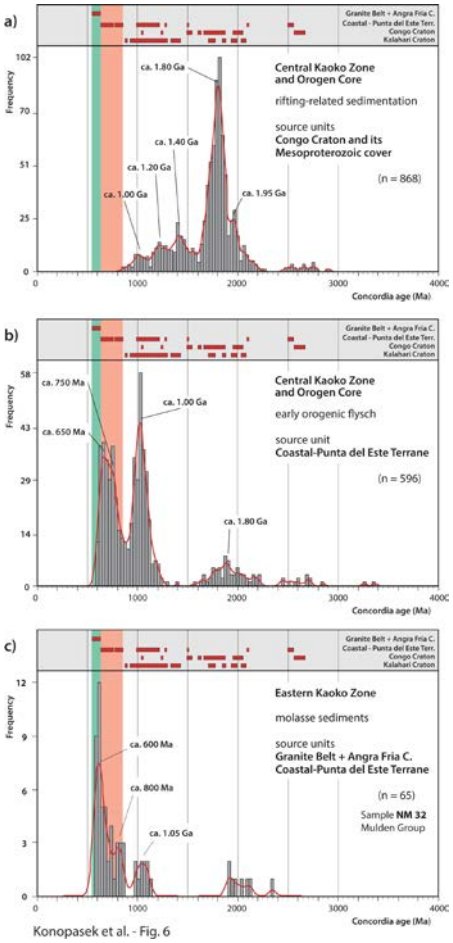

Figure 6. a) U–Pb detrital zircon data for the sample NM 32 representing the late orogenic molasse sediments of the Mulden Group. b) Pooled U–Pb detrital zircon data for the metasedimentary samples of this study and from Konopásek et al. (2014) interpreted as the early orogenic flysch of the Kaoko Belt. c) Pooled U–Pb detrital zircon data for the rifting-related sedimentation in the lower part of the Neoproterozoic cover of the Congo Craton in the Kaoko Belt (data from this study, Konopásek et al., 2014 and Goscombe et al., 2005). Upper part of each figure is a bar diagram showing distribution of protolith ages in potential source areas. In the detrital zircon age record, the time interval between *ca.* 630 and 850 Ma shown as a red verical bar represents a typical signal of the Punta del Este–Coastal Terrane, whereas the interval between *ca.* 550 and 630 Ma shown in green represents a typical signal of the plutonic activity in the Aiguá, Pelotas, Florianópolis and Angra Fria batholiths and of the syn-collisional magmatism in the Coastal Terrane.

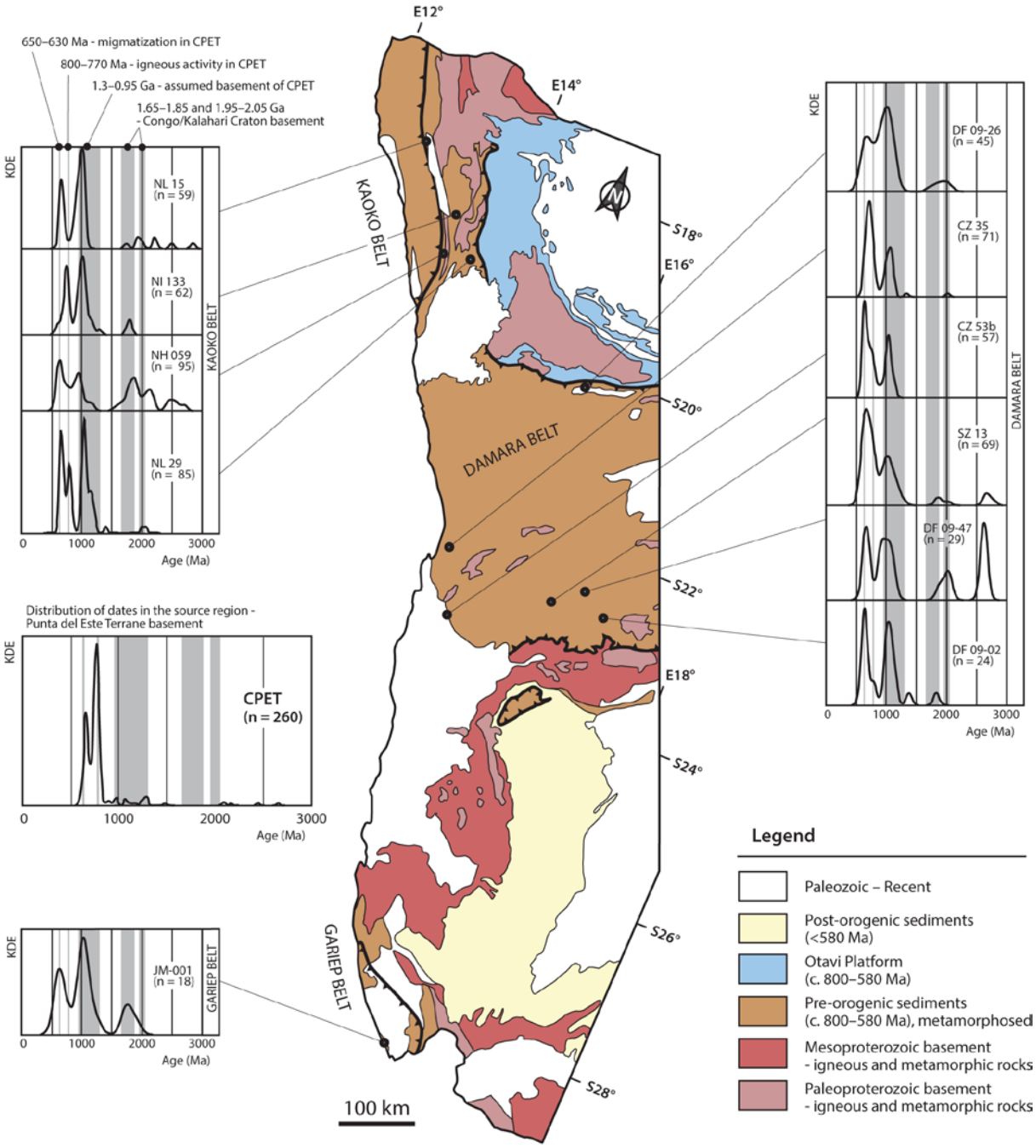

Konopasek et al. - Fig. 7

Figure 7. Position and the detrital zircon record of the samples representing the early orogenic flysch covering the rifting-related sediments of the Kaoko, Damara and Gariep belts. The samples from the Damara Belt are from Foster et al. (2015), the sample from the Gariep Belt is from Basei et al. (2005) and the samples from the Kaoko Belt are from this study and

from Konopásek et al. (2014). The diagram marked CPET represents the distribution of the dates obtained by SIMS dating of single zircons in meta-igneous rocks of the Punta del Este Terrane basement interpreted as the source region for the early orogenic flysch sediments (data from Lenz et al., 2011 and Masquelin et al., 2012). The grey bands underlying the data diagrams show the timing of zircon-forming events in the particular tectonic units and these events and units are explained in the upper left part of the figure. Abbreviations: CPET – Punta del Este–Coastal Terrane; KDE – Kernel density estimate; n – number of data. The simplified map of tectonic units does not show the distribution of syn- to post-orogenic granites in the particular metamorphic belts.